

Structural and dielectric properties of $\text{Ba}_{0.95}\text{Bi}_{0.05}\text{Ti}_{1-x}\text{Fe}_x\text{O}_3$ ceramics at $x=0.0, 0.1$ and 0.2 prepared by solid state method

Najwa Gouitaa^{1,*}, Taj-dine¹, Lamcharfi, Lamfadal Bouayad¹, Farid Abdi¹ and Mohammed Naciri Bennani²

¹Electrical Engineering Department. Signals, Systems and Components Laboratory (LSSC). Fez, Morocco.

²Chemistry-biology applied to the environment laboratory Materials and applied catalysis team. Meknes, Morocco

Abstract: The $\text{Ba}_{0.95}\text{Bi}_{0.05}\text{Ti}_{1-x}\text{Fe}_x\text{O}_3$ ceramics at ($x=0.0, 0.1$ and 0.2) were prepared by the solid-state reaction method. The effect of iron substitution on structural and dielectric properties of $\text{Ba}_{0.95}\text{Bi}_{0.05}\text{TiO}_3$ ceramic was studied. These compounds are found to crystallize in only tetragonal phase for $x = 0.0$ and 0.1 and the mixture of tetragonal and hexagonal phases for $x = 0.2$. The dielectric properties of $\text{Ba}_{0.95}\text{Bi}_{0.05}\text{Ti}_{1-x}\text{Fe}_x\text{O}_3$ ceramics at $x=0.0, 0.1$ and 0.2 of Fe -doping concentration. The dielectric measurements as a function of temperature and frequency are studied and showed two diffuse phase transition and relaxation phenomena. The evolution of dielectric permittivity as a function of the frequency of undoped $\text{Ba}_{0.95}\text{Bi}_{0.05}\text{TiO}_3$ show a relaxation phenomenon for which is displaced to the higher frequencies accompanied by a decrease in dielectric constant when x increase. The Complex impedance Cole-Cole plots showed a negative temperature coefficient of resistivity (NTCR) behavior of the $\text{Ba}_{0.95}\text{Bi}_{0.05}\text{Ti}_{1-x}\text{Fe}_x\text{O}_3$ materials and increased in grain and grain boundaries resistivity. The relaxation behavior in the test materials is found to be of non-Debye type.

Keywords: $\text{Ba}_{0.95}\text{Bi}_{0.05}\text{Ti}_{1-x}\text{Fe}_x\text{O}_3$ ceramics Solid state, structural, dielectric properties, phase transition, Complex impedance.

Introduction

During the recent decade, multiferroic materials have attracted the great attention of researchers over the last decade because of interest in their potential at information storage, MERAM, spintronics etc^{1,2}.

The tetragonal perovskite BaTiO_3 with a Curie temperature (T_c) of 120°C , has been adapted as a popular candidate in the research of multiferroic materials is the most ferroelectric material which exhibits a high dielectric constant, low dielectric loss and good piezoelectric, pyroelectric and ferroelectric properties³. To achieve a magnetic ordering in the semiconducting BaTiO_3 , the magnetic ions can be doping into it for extending the field of its application⁴. The Fe doped BaTiO_3 has been reported to have magnetic ordering, where the Fe ions substitute into the Ti^{4+} sites^{5,6}. However, the major problems of earlier BTFO ceramic are the high Curie temperature which is displaced to the higher temperature with increasing of Fe doping contents⁷ and the low dielectric constant which limited their application. As an effective approach in altering or improving physical

properties, co-doping into ABO_3 compounds at A-site and B-site is widely used. It has been reported that the substitution of Bi^{3+} ions into the Ba^{2+} sites ($\text{Ba}_{1-x}\text{Bi}_x\text{TiO}_3$) achieves a maximum dielectric constant at $x=0.05$ ⁸. The structure of $\text{Ba}_{1-x}\text{Bi}_x\text{TiO}_3$ ($x \leq 0.1$) was reported to be of a tetragonal phase^{9,10}.

The present study is intended to study the influence of Fe doping on structural and dielectric properties of $\text{Ba}_{0.95}\text{Bi}_{0.05}\text{Ti}_{1-x}\text{Fe}_x\text{O}_3$ solid solution at $x=0.0, 0.1$ and 0.2 Fe -doping concentration.

Experimental

The $\text{Ba}_{0.95}\text{Bi}_{0.05}\text{Ti}_{1-x}\text{Fe}_x\text{O}_3$ ceramics at ($x=0.0, 0.1$ and 0.2) were prepared by the conventional solid-state method. The BaCO_3 , Bi_2O_3 , TiO_2 and Fe_2O_3 compounds were weighted in stoichiometric proportion and milled under acetone for 4h. After that, the powders were dried at 70°C for 48h. The dried powders were mixed using agate mortar and pestle for 30 min and then placed in an alumina nacelle for calcination in air at 1100°C for 4h. The crystal structure of the product ($\text{Ba}_{0.95}\text{Bi}_{0.05}\text{Ti}_{1-x}\text{Fe}_x\text{O}_3$) was

*Corresponding author: Najwa Gouitaa

E-mail adresse: najwa.gouitaa@gmail.com

DOI: <http://dx.doi.org/10.13171/mjc8319050305ng>

Received February 11, 2019

Accepted March 23, 2019

Published May 3, 2019

characterized by X-ray diffraction (XPERT-PRO with Cu K α radiation with $\lambda=1.5406\text{\AA}$). The calcined powders were pressed into pellets and sintered in air at 1200 °C for 6h. The dielectric properties as a function of frequency and temperature were tested with Agilent E4980A (20Hz-2MHz).

Results and discussion

X-ray diffraction results

The Fig.1a shows the XRD patterns of Ba_{0.95}Bi_{0.05}Ti_{1-x}Fe_xO₃ ceramics for x=0.0, 0.1 and 0.2. calcined at 1100°C/4h. The synthesized samples show a pure perovskite structure with no secondary

phases detected. For x=0.0 and 0.1 only a tetragonal phase was observed¹¹. While the X-ray analysis of Fe doping Ba_{0.95}Bi_{0.05}TiO₃ at x=0.2 showed the coexistence of tetragonal and hexagonal phase. The tetragonal (101) peak and hexagonal (104) peak were zoomed in Fig.1b. The X-ray analysis of these peaks reveals that the (104) hexagonal peak appears at x=0.2 while the intensity of (101) tetragonal peak decreases with the increase of Fe content. So the Fe additive stabilizes the hexagonal phase in Ba_{0.95}Bi_{0.05}TiO₃ ceramic and removes the tetragonal phase formation. The (101) peak shifted to higher angles for all samples which can be attributed to the presence of Fe⁴⁺ with the ionic radius [r(Fe⁴⁺) = 0.585 Å] smaller than the ionic radius of Ti⁴⁺ (ri(Ti⁴⁺) = 0.605 Å)¹²

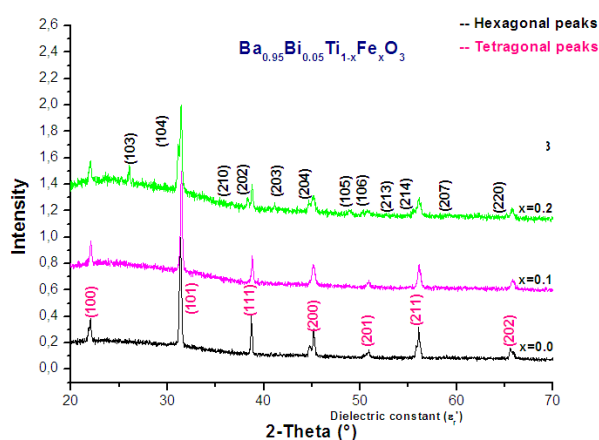


Figure 1a. XRD patterns of Ba_{0.95}Bi_{0.05}Ti_{1-x}Fe_xO₃ ceramics for x=0.0, 0.1 and 0.2

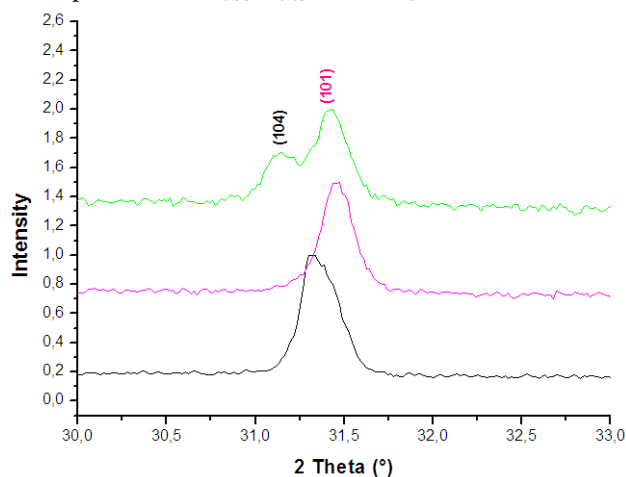


Figure 1b. XRD peaks (101) for the tetragonal phase and (104) for the hexagonal phase of Ba_{0.95}Bi_{0.05}Ti_{1-x}Fe_xO₃ ceramics for x=0.0, 0.1 and 0.2.

Rietveld refinement

To obtain more detailed information about the crystallographic structure of Ba_{0.95}Bi_{0.05}Ti_{1-x}Fe_xO₃ solids for x=0.0, 0.1 and 0.2, we performed full pattern matching the refinement of the XRD spectra using the Full prof program package as shown in Fig. 2. A Pseudo-Voigt function described the peak shapes. From the results of the refinement (Fig. 2 and Table.1), only one phase is detected for x =0.0 and

x=0.1 with P 4 m m space group while two phases are found at x=0.2 prepared sample with P6₃/m m c space group. There is no other observable impurity phase in the system. According to the refinements, most of the Fe ions are believed to be embedded in Ba_{0.95}Bi_{0.05}TiO₃ crystal lattice and substitute for Ti ions, so there is no obvious secondary phase observed in diffraction patterns. A good agreement between the observed and calculated patterns was

obtained with $R_p \leq 8.59\%$, $R_{wp} \leq 13.4\%$ and chi-

squared ($\chi^2 \leq 3.85$ for all ceramics.

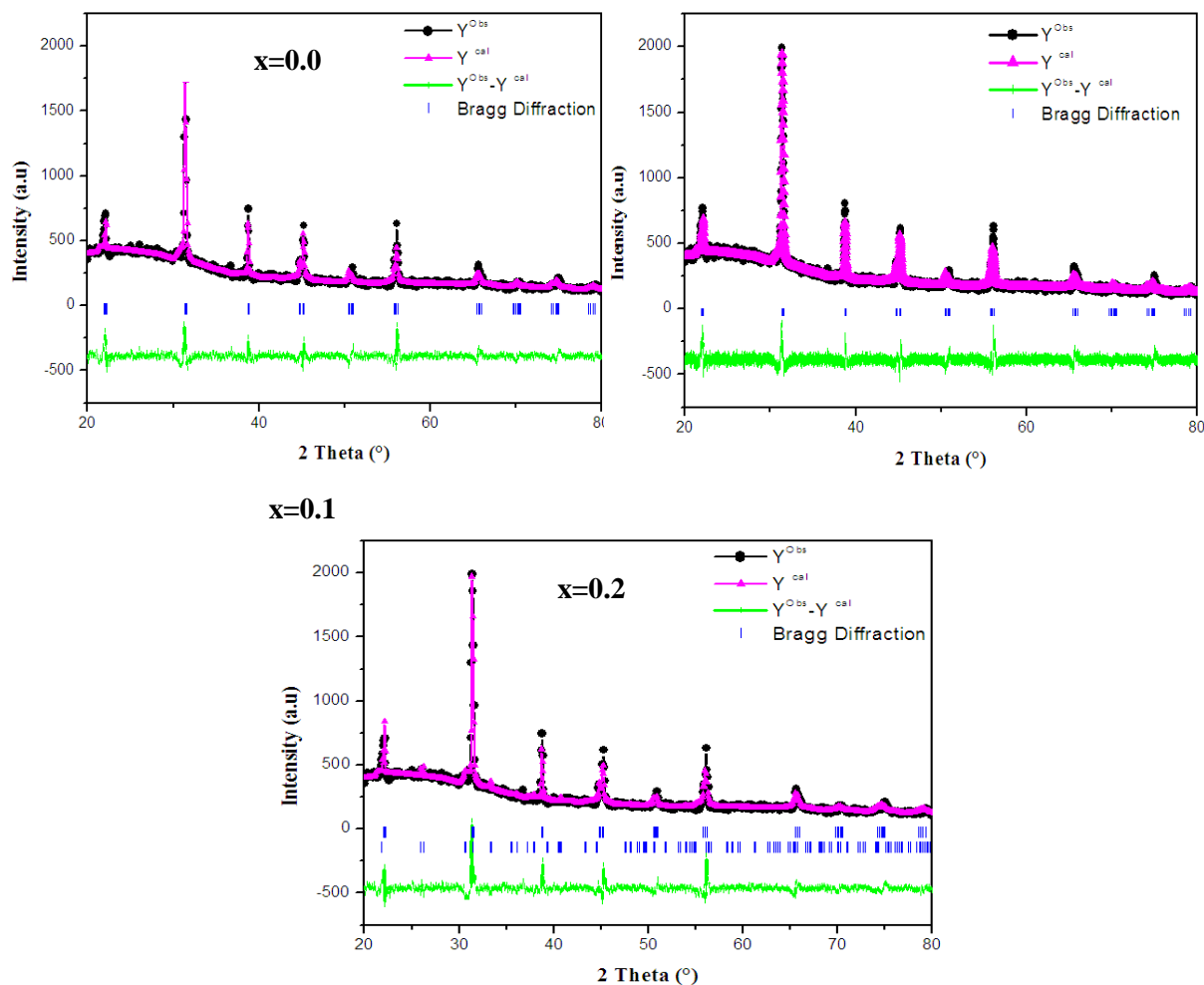


Figure 2. Rietveld refinement of $Ba_{0.95}Bi_{0.05}Ti_{1-x}Fe_xO_3$ ceramics for $x=0.0, 0.1$ and 0.2 .

Table 1. Refined structural parameters of $Ba_{0.95}Bi_{0.05}Ti_{1-x}Fe_xO_3$ ceramics for $x=0.0, 0.1$ and $0.2x$.

x	0.0 Tetragonal phase	0.1 Tetragonal phase	0.2 Hexagonal phase	Tetragonal phase
R- factor	$R_p = 6.14$ $R_{wp} = 8.60$ $\chi^2 = 1.73$	$R_p = 7.43$ $R_{wp} = 10.20$ $\chi^2 = 2.65$	$R_p = 8.59$ $R_{wp} = 13.4$ $\chi^2 = 3.85$	$R_p = 5.96$ $R_{wp} = 7.53$ $\chi^2 = 1.34$
Lattice constants (\AA)	$a = 4.012245$ $c = 4.047829$	$a = 3.9999$ $c = 4.0170$	$a = 5.8390$ $c = 13.7608$	$a = 4.00524$ $c = 4.01916$
Volume (\AA^3)	65.162	64.2688	406.3087	64.475
Space group	P 4 m m	P 4 m m	P 63 m m c	P 4 m m

Dielectric properties

The evolution of the real part of the dielectric permittivity (ϵ') as a function of temperature (R. T to $600\text{ }^\circ\text{C}$) at various frequencies (5 KHz to 2 MHz) for the selected $Ba_{0.95}Bi_{0.05}Ti_{1-x}Fe_xO_3$ composition is represented in Fig. 3. Two dielectric peaks were observed for all the samples. They originated from a tetragonal ferroelectric phase to orthorhombic ferroelectric phase at T_{T-O} then to a cubic paraelectric

phase at T_{O-c} ^{13,14}. As it is indicated in Table 2, the T_{T-O} phase transition shifted to the higher temperature with the increase of Fe substitution for all frequencies due to the increase of hexagonal phase which is known as a ferromagnetic phase¹⁵. While the T_{O-c} shifted to the lower temperature for all the frequencies with arise of Fe content indicating the big effect of Fe doping on dielectric proprieties of $Ba_{0.95}Bi_{0.05}TiO_3$ ceramic.

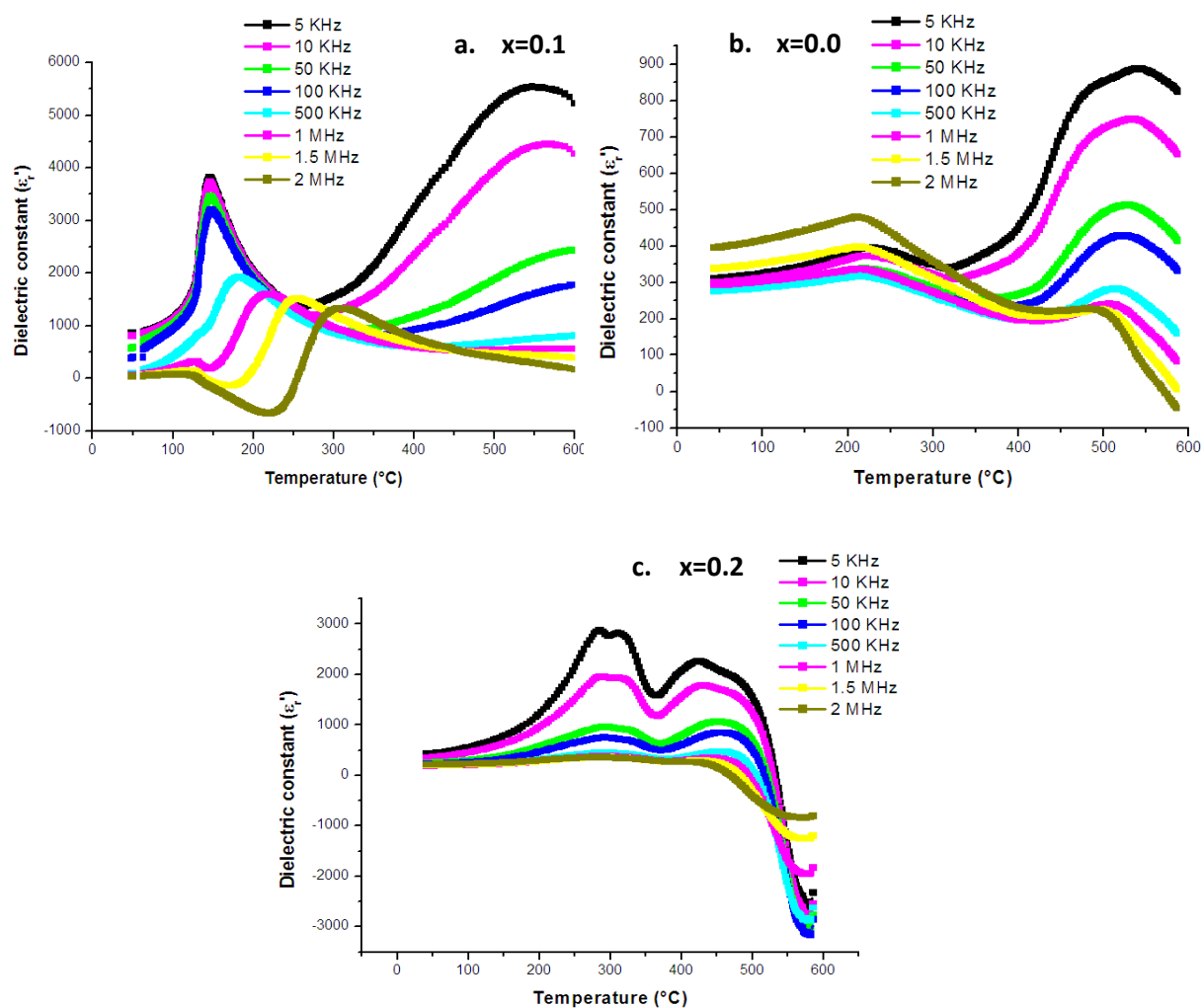


Figure 3. Dielectric constant dependent temperature at different frequencies of $\text{Ba}_{0.95}\text{Bi}_{0.05}\text{Ti}_{1-x}\text{Fe}_x\text{O}_3$ ceramics for $x = a. 0.0, b. 0.1$ and $c. 0.2$.

Table 2. T_m , T_{T-O} , T_{O-c} , $\epsilon_{1,max}$ and $\epsilon_{2,max}$ values at different frequencies of $\text{Ba}_{0.95}\text{Bi}_{0.05}\text{Ti}_{1-x}\text{Fe}_x\text{O}_3$ ceramics.

	Fréquence (KHz)	T_m (°C)	T_c (°C)	T_{T-O} (°C)	$\epsilon_{1,max}$	$\epsilon_{2,max}$
0.0	5	---	145	535	3846	5540
	50	---	145	594	3505	2427
	100	---	145	>600	3247	1828
	500	175		>600	1947	---
	1000	212		>600	1606	---
	2000	302		>600	1350	---
0.1	5	235		540	401	890
	50	232		530	342	516
	100	225		516	342	433
	500	227		511	323	288
	1000	226		508	390	250
	2000	215		491	482	234
0.2	5	283		245	2326	2903
	50	285		427	1755	953
	100	287		449	846	715
	500	289		457	511	481
	1000	289		451	344	413
	2000	386		445	178	403

The phases transition in our sample presents a relaxor-like behavior due to the relaxation process associated with defect dipoles such as the oxygen-vacancy and the valence fluctuation of Fe ions (between Fe^{3+} and Fe^{2+})¹⁶. Literature reports that the deviation from oxygen stoichiometry leads to valence fluctuation of Fe ions from Fe^{3+} to Fe^{2+} state in BaTiO_3 , resulting in a high conductivity^{17,18}. In this case, the short-range hopping of oxygen vacancy and valence variation of iron ions, similar to the reorientation of the dipole, lead to a dielectric anomaly reflected in the increase of the two dielectric permittivity values ($\epsilon_{1,\text{max}}$, and $\epsilon_{2,\text{max}}$) at $x=0.1$ and then the decrease of these values at $x=0.2$ for all the frequencies (Table.2). Generally, in perovskite ferroelectric compounds, oxygen vacancies are considered as one of the mobile charge carriers, and mostly in titanates, the ionization of oxygen vacancies creates conduction electrons, a process which is defined by Kröger Vink notation¹⁹.

The dielectric properties are studied by measuring the constant dielectric dependent on the frequency at different temperature as shown in Fig. 4 for $\text{Ba}_{0.95}\text{Bi}_{0.05}\text{Ti}_{1-x}\text{Fe}_x\text{O}_3$ ceramics with $x=$ a. 0.0, b. 0.1 and c. 0.2. For $\text{Ba}_{0.95}\text{Bi}_{0.05}\text{TiO}_3$ compound (Fig 3a), the dielectric constant presents a particular evolution with the increase of frequency. ϵ_r , max reaches a maximum with the increase of frequency and then decreases and reaches a minimum. This maximum value ϵ_r , max increases with the increase of temperature to 8000 for $T^\circ = 160^\circ\text{C}$ and then decrease. For Fe-doped $\text{Ba}_{0.95}\text{Bi}_{0.05}\text{TiO}_3$ at $x = 0.1$ and 0.2 (Fig. 3b and 3c) we found that the relaxation phenomenon was eliminated or displaced to the high frequencies. Moreover, classical ferroelectric behavior is observed. So the Fe substitution eliminates the relaxation phenomenon and decreases the dielectric constant of the samples (Fig. 4b and 4c). Thus the drastic reductions in ϵ_r value upon Fe substitution can be attributed to the creation of oxygen vacancy due to Fe^{3+} ions replacing Ti^{4+} ions. Such oxygen vacancy leads to the breaking of Ti-O bonds and affects the dielectric constant²⁰.

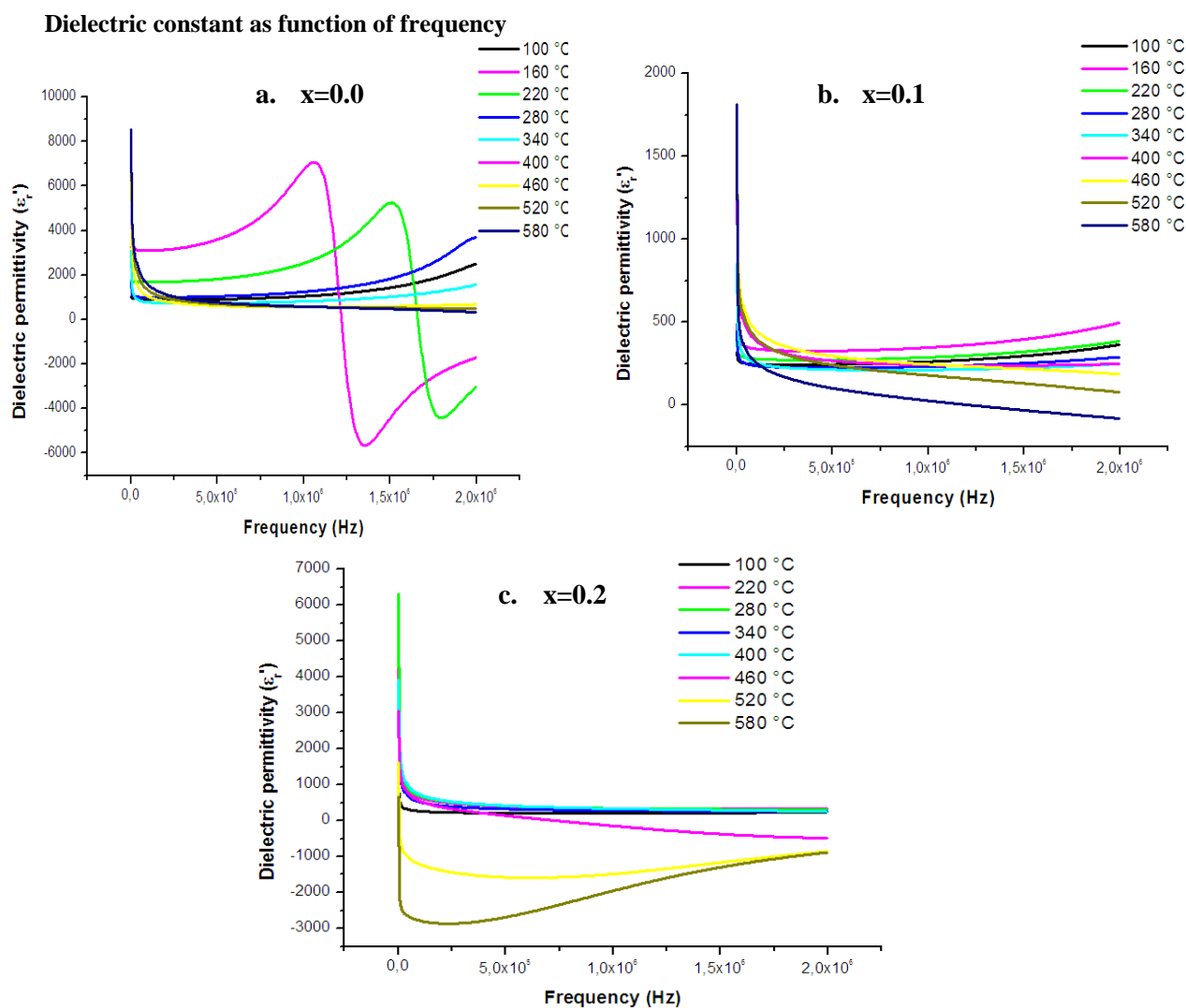


Figure 4. Dielectric constant dependent frequency at different frequencies of $\text{Ba}_{0.95}\text{Bi}_{0.05}\text{Ti}_{1-x}\text{Fe}_x\text{O}_3$ ceramics for $x=$ a. 0.0, b. 0.1 and c. 0.2.

Electric properties

To understand the mechanism of the relaxation behavior in $\text{Ba}_{0.95}\text{Bi}_{0.05}\text{Ti}_{1-x}\text{Fe}_x\text{O}_3$ ceramics the Cole-Cole plots from 100 °C to 400 °C of measurement temperature was studied. At the impedance spectrum study of $\text{Ba}_{0.95}\text{Bi}_{0.05}\text{Ti}_{1-x}\text{Fe}_x\text{O}_3$ ceramic at $x=0.1$ (Fig.5), all the curves showed a tendency to bend towards the abscissa to form semicircles with their centers below the real axis, having comparatively larger radii. For all ceramics (data not shown), the radii decrease with the increase of temperature, indicating negative temperature coefficient of resistivity (NTCR) behaviour of the materials^{21,22}, generally found in case of semiconductors and at the same time showing a non-ideal Debye type behavior²³. This nonideal behavior could be attributed to several factors such as grain orientation, grain boundary, stress-strain phenomena, and atomic defect distribution²⁴. The

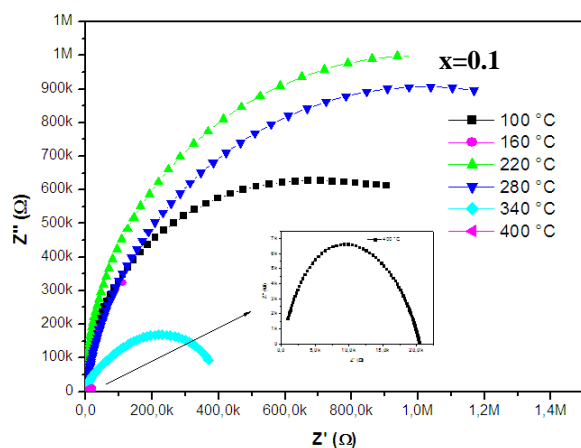


Figure 5. Complex impedance of $\text{Ba}_{0.95}\text{Bi}_{0.05}\text{Ti}_{1-x}\text{Fe}_x\text{O}_3$ ceramics for $x=$ a. 0.0, b. 0.1 and c. 0.2 at different temperature.

In order to co-relate the electrical parameters with the conduction process in the Fe-doped $\text{Ba}_{0.95}\text{Bi}_{0.05}\text{TiO}_3$ ceramics, the ac conductivity is studied as a function of frequency. For Fig.7a two distinct regions are observed in the conductivity spectra of $\text{Ba}_{0.95}\text{Bi}_{0.05}\text{TiO}_3$ sample. At lower frequencies, the conductivity is almost constant. This is the evidence for the frequency independent nature of the conductivity which represents the dc conductivity. While at high frequencies, the conductivity exhibits frequency dispersion due to the tremendous increase of the mobility of charge carriers in the materials²⁶. In the high-frequency region, the conductivity increases with the frequency. At $x=0.1$ and 0.2 we observe two regions. The variation of conductivity in the low-frequency region is attributed to the polarization effects at the electrode and electrolyte interface. As the frequency reduces, more and more the charge accumulation

impedance spectrum showed semicircles at and above the 520 °C, 400°C, 400 °C temperatures for $x=0.0, 0.1, 0.2$ respectively.

According to the impedance spectrum data obtained of $\text{Ba}_{0.95}\text{Bi}_{0.05}\text{Ti}_{1-x}\text{Fe}_x\text{O}_3$ ceramics at $x=0.0, 0.1$ and 0.2 at 400°C of measurement temperature, all the samples, are represented by a number of elements, one R/C and other R/CPE connected in series (Fig. 6). The plots and Tab.3 show that the grain resistivity increase with increases of Fe contents while the grain boundaries resistivity decreases as the concentration of Fe^{3+} increased from 0.0 to 0.2. The Complex impedance spectrum of $x=0.1$ and 0.2 samples show the presence of an arc of a circle with the center below the real axis indicating the contribution of the ceramic's boundaries, grain boundaries and electrode-interfaces²⁵.

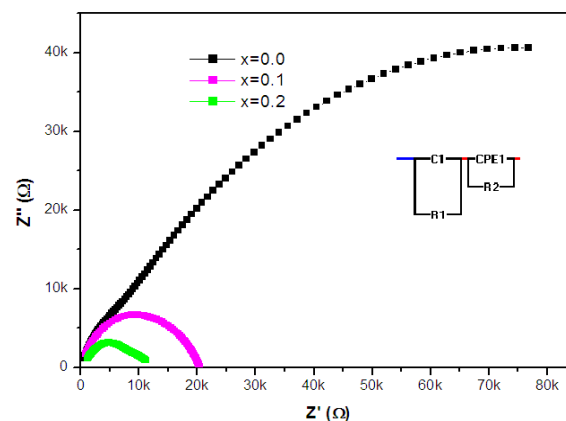


Figure 6. Complex impedance plots of $\text{Ba}_{0.95}\text{Bi}_{0.05}\text{Ti}_{1-x}\text{Fe}_x\text{O}_3$ ceramics for $x= 0.0, 0.1$ and 0.2 measured at 400 °C.

occurs at the electrode and electrolyte interface and hence, drop in conductivity. At high frequencies, the conductivity σ_{ac} (Fig. 7) plots to change their slopes as a function of frequency with increasing Jonscher's exponent pointing due to the change of diffusive charge carrier transport to the hopping one²⁷.

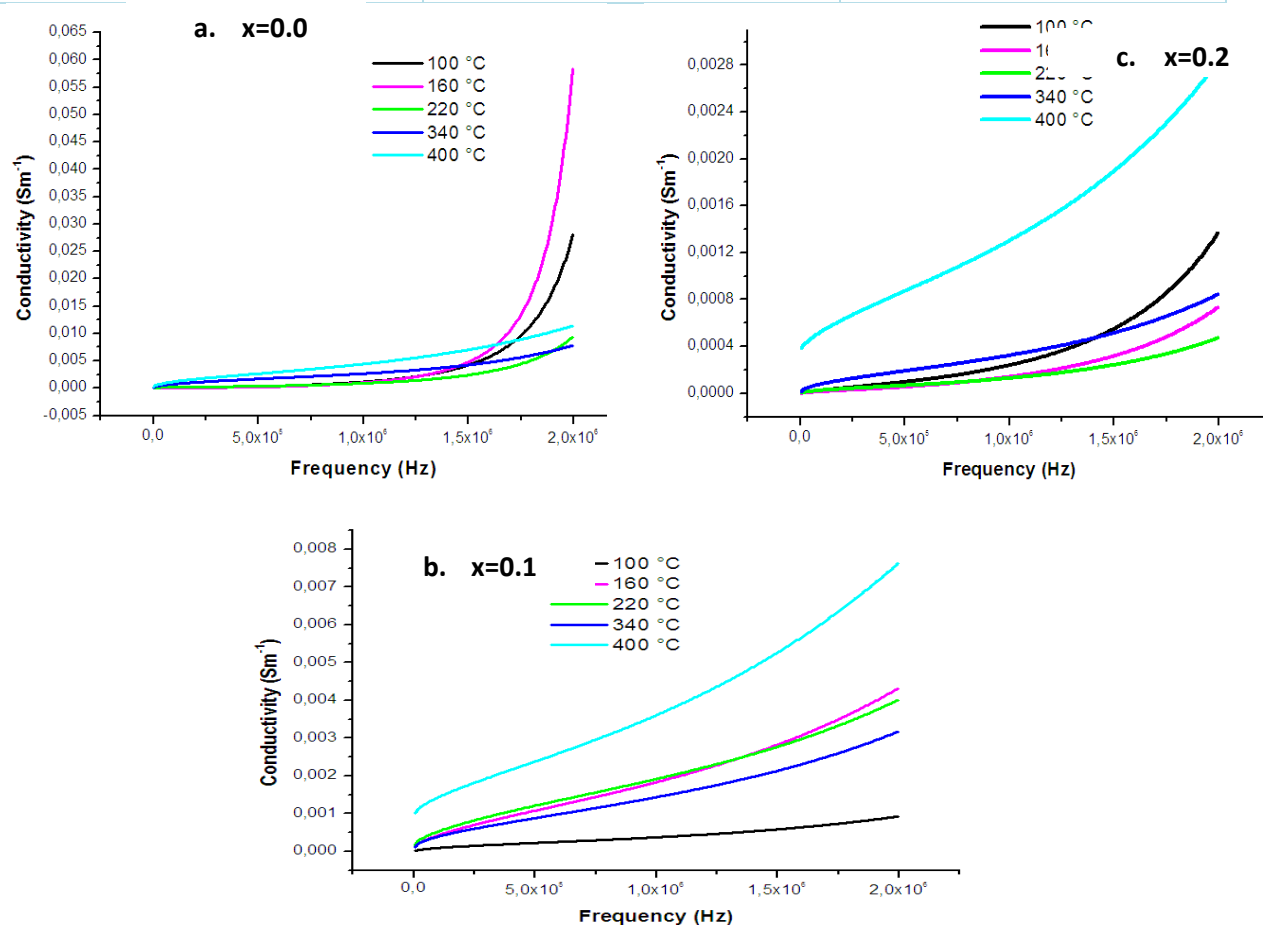
The frequency dependence of conductivity or so-called universal dynamic response (UDR) of ionic conductivity is related by a simple expression given by Jonscher's power law²⁸:

$$\sigma_{\omega} = \sigma_0 + A \omega^s$$

Where, σ_{ω} , is the ac conductivity, σ_0 is the limiting zero frequency conductivity σ_{dc} , A is a pre-exponential constant, $\omega = 2\pi f$ is the angular frequency, and s is the power law exponent, where $0 < s < 1$.

Table 3. Grain and grain boundaries resistivity of different composition of $\text{Ba}_{0.95}\text{Bi}_{0.05}\text{Ti}_{1-x}\text{Fe}_x\text{O}_3$ ceramics.

Composition of $\text{Ba}_{0.95}\text{Bi}_{0.05}\text{Ti}_{1-x}\text{Fe}_x\text{O}_3$	Grain boundaries resistivity R_{GB} (Ω)	Grain resistivity R_{G} (Ω)
$x=0.0$		587,24063
$x=0.1$	20378,19748	905,50546
$x=0.2$	11164,30333	1215,43351

**Figure 7.** Ac conductivity plots of $\text{Ba}_{0.95}\text{Bi}_{0.05}\text{Ti}_{1-x}\text{Fe}_x\text{O}_3$ ceramics for $x=$ a. 0.0, b. 0.1 and c. 0.2 measured at different temperature

Conclusion

The effect of Fe substitution on structural and dielectric properties of $\text{Ba}_{0.95}\text{Bi}_{0.05}\text{TiO}_3$ ceramics at $x=0.0$, 0.1 and 0.2 was studied. The X-ray diffractions showed the formation of only the tetragonal phase for $x=0.0$ and 0.1 while the coexistence of tetragonal and hexagonal phase for $x=0.2$ is observed. The dielectric measurement showed the existence of two maxima in the dielectric constant as a function of temperature corresponding to the two-phase transition. The first one is the phase transitions from a cubic paraelectric to a tetragonal ferroelectric at the Curie temperature ($T_{\text{C}}/T_{\text{m}}$) while

the second one is from a tetragonal to an orthorhombic ferroelectric at $T_{\text{T-O}}$. This temperature shifted to lower temperature with

increase of Fe doping. The relaxation behavior present in all the samples is related to the defect dipoles such as the oxygen-vacancy and the valence fluctuation of Fe ions (between Fe^{3+} and Fe^{2+}). The complex impedance spectroscopy approved the grain and grain boundary contributions towards electrical conductivity and the presence of a non-Debye type of relaxation in the majority of the materials. The frequency response of the conductivity for the test materials follows the Jonscher's power law. The Cole-Cole plots show that the electrical resistivity of

the sample increases as the concentration of Fe^{3+} increased from 0.0 to 0.2 and the relaxation behavior in the test materials is found to be of non-Debye type.

References

- 1- K.F. Wang, J.-M. Liu and Z.F. Ren, *Adv. Phys*, **2000**, 58,321.
- 2- Z.H. Chi, C.J. Xiao, S.M. Feng, F.Y. Li, C.Q. Jin, X.H. Wang, R.Z. Chen and L.T. Li, *J. Appl. Phys*, **2005**, 98, Paper No. 103519.
- 3- M.M. Vijatovic, J.D. Bobic and B.D. Stojanovic, *Sci. Sinter*, **2008**, 40, 155.
- 4- Y.H. Chu, L.W. Martin, M.B. Holcomb, M. Gajek, S.J. Han, Q. He, N. Balkar, C.H. Yang, D. Lee, W. Hu, Q. Zhan, P.L. Yang, A. Fraile Rodeiguez, A. Scholl, S.X. Wang and R. Ramesh, *Nat. Mater*, **2008**, 7, 478.
- 5- S.Y. Qiu, W. Li, Y. Liu, G.H. Liu, Y.Q. Wu, N. Chen, *Trans. Nonferrous Met. Soc. China*, **2010**, 20, 1911.
- 6- G.P. Du, Z.J. Hu, Q.F. Han, X.M. Qin, W.Z. Shi, *J. Alloys Compd*, **2010**, 492, L79.
- 7- I. N. Apostolova, A. T. Apostolov, Safa Golrokh Bahoosh and Julia M. Wesselinowa. *Journal of applied physics*, **2013**, 113, 203904.
- 8- X.P. Jiang, M. Zeng, K.W. Kowk, H.L.W. Chan, *Key Eng. Mater*, **2007**, 334, 977.
- 9- Widi Yansen, Kadek Juliana Parwanta, Hadiyawarman, Deokhyeon Kim, Younmi Gwan, Jaeyeong Kim, Chunli Liu, Chang Uk Jung and Bo Wha Lee. *Journal of the Korean Physical Society*, , **2013**, pp. 306-309
- 10- N. Vittayakorn, *J. Appl. Sci. Res*, **2006**, 2 (12), 1319.
- 11- QIU Shen-yu, LI Wang, Liu Yu, Liu Gui-hua, Wu Yi-qiang and Chen Nan. *Trans. Nonferrous Met. Soc. China*, **2010**, 20, 1911-1915.
- 12- P.Zhang, D.Grinting, S.Yu, N.Nghia, N.Dang and V.Lam. *J.Appl.Phys*, **2012**, 112, 013909.
- 13- Poonam Kumari, Radheshyam Rai, Seema Sharma and M. A. Valente. *Journal of advanced dielectrics*, **2017**, 1750034 (10 pages).
- 14- Fayçal Bourguiba, Ah. Dhahri, Tarek Tahri, J. Dhahri, N. Abdelmoula, K. Taibi, E.K. Hlil. *Journal of Alloys and Compounds*, **2016**, 675, 174e182.
- 15- N. Gouitaa, T. Lamcharfi, MF. Bouayad, F. Abdi, N.S. Echatoui and N. Hadi. *Asian Journal of Chemistry*, **2017**, 2143-214.
- 16- X.K. Wei, Y.T. Su, Y. Sui, Z.X. Zhou, Y. Yao, C.Q. Jin and R.C. Yu, *J.Appl. Phys*, **2013**, 102, 242910.
- 17- P.R. Mandal and T.K. Nath. *J. Alloys Compd*, **2015**, 628, 379e389.
- 18- Yuwen Liu, Yongping Pu, Zixiong Sun and Qian Jin. *Mater. Res. Bull*, **2015**, 70, 195e199.
- 19- C. Ang, Z. Yu, Z. Jing, P. Lunkenheimer and A. Loidl. *Phys. Rev*, **2000**, B 61, 3922.
- 20- B. Deka, S. Ravi, A. Perumal and D. Pamu, *Physica B*, **2014**, 448, 204.
- 21- P.Ouyang, H. Zhang, D.Xue and Z.Li. *Materials in Electronics*. October, **2013**, pp 3932–3939.
- 22- D. Xue, H. Zhang, Y. Li, Y. Liu and Z. Li. *Journal of Materials Science: Materials in Electronics*. July, **2012**, pp 1306–1312.
- 23- H. Khelifi, I.Zouari, A. Al-Hajry, N. Abdelmoula, D. Mezzane and H. Khemakhem. *Ceramics International*, **2015**, 41, 12958– 12966.
- 24- N.Gouitaa, T.Lamcharfi, Mf.Bouayad, F.Abdi, N.Hadi. *Journal of Materials Science: Materials in Electronics*, **2018**, p6797-6804. 8p.
- 25- H. D. Li, C. D. Feng, and P. H. Xiang. *Jpn. J. Appl. Phys*, **2003**, pp.7387 7391.
- 26- Shujahadeen B. Aziz, Omed Gh. Abdullah, Salah R. Saeed and Hameed M. Ahmed. *Int. J. Electrochem. Sci*, **2018**, 13, 812.
- 27- H. Khelifi, I.Zouari, A. Al-Hajry, N. Abdelmoula, D. Mezzane and H. Khemakhem. *Ceramics International*, **2015**, 41, 12958–12966.
- 28- A. K. Jonscher. *Journal of Materials Science* August, **1981**, pp 2037–2060.